Interface two-dimensional metallicity but lack of superconductivity in heterobonded semiconductors: ZnS/Si and GaP/Si

S. H. Rhim,[1,*] R. Saniz,[1,†] and A. J. Freeman[1,2]
[1]*Department of Physics and Astronomy, Northwestern University, Evanston, Illinois 60208, USA*
[2]*Department of Materials Science and Engineering, Northwestern University, Evanston, Illinois 60208, USA*
(Received 20 May 2008; revised manuscript received 7 November 2008; published 22 January 2009)

As a follow up to our finding that CuCl/Si superlattices exhibit metallicity at the interfaces and possibly superconductivity, we explore other semiconductor superlattices for the same properties and present here our results for ZnS/Si and GaP/Si superlattices. As found for the CuCl/Si superlattices, both the ZnS/Si and GaP/Si superlattices exhibit two-dimensional metallicity at their interfaces, as shown by their band structures, Fermi surfaces, and charge-density distributions. Furthermore, to gauge any possible superconductivity, the McMillan-Hopfield electron-phonon coupling constant, λ, is calculated using the rigid muffin-tin approximation. Electron-phonon coupling is observed mostly at the interfaces but it is not strong enough to cause superconductivity at a finite temperature as estimated using the McMillan formula for T_c. This contrasts greatly with the CuCl/Si superlattices, in which electron-phonon coupling is strong enough to indicate superconductivity.

DOI: 10.1103/PhysRevB.79.045313 PACS number(s): 73.20.−r, 79.60.Jv

I. INTRODUCTION

Heterostructures and interfaces are currently intensively studied topics in condensed-matter physics, motivated by their intriguing physics and also as part of the enormous effort in searching for novel device applications materials. Advances in experimental techniques such as synthesis and epitaxial growth, which have a long history since the 1970s,[1] nowadays enable the study of heterostructures and interfaces at the atomic scale.[2,3] In its early stages, this research was mostly on semiconductors which combined direct and indirect band-gap III-V and group IV semiconductors. Current studies on heterostructures are not restricted to semiconductors but also include perovskite oxides and combinations or superlattices of metal-semiconductors, exhibiting a rich variety of properties such as ferroelectricity, high mobility, and superconductivity at two-dimensional (2D) interfaces.[3–5]

In 1985, shortly before the discovery of superconductivity in the cuprates, Mattes and Foiles[6] (MF) reported nearly ideal diamagnetism between 60 and 150 K in CuCl grown epitaxially on Si (111). These results followed the great attraction that CuCl drew from the physics community in the late 1970s due to possible superconductivity under pressure,[7,8] which would be a sign of excitonic superconductivity[9] proposed by Little[10] and Ginzburg[11] in the early 1960s. Mattes[12] later suggested that the CuCl/Si results could be understood as a manifestation of an excitonic mechanism of superconductivity,[13,14] which can be realized in a dielectric-metal-dielectric sandwich structure. Those results were neither reproduced nor confirmed thereafter. However, the MF results called for a more thorough understanding of the properties of the CuCl/Si system. Preliminary *ab initio* calculation results in 1986 by Yu and Freeman[15] showed that 2D interface metallicity was plausible. Recently, we reported 2D interface metallicity and possible phonon-mediated superconductivity (T_c=0.03–4.4 K) in CuCl/Si superlattices.[16] These results lead naturally to the question of how do other similar semiconductor superlattices behave regarding those properties.

To answer this question, ZnS and GaP interfaces with Si were investigated and their properties are reported here. These have similar lattice constants to those of Si and CuCl. On the other hand, while CuCl is a strongly ionic (I-VII) compound, ZnS and GaP are II-VI and III-V semiconductors, respectively, which would have different polarity at the interface from CuCl and Si. Results on the electronic structure of ZnS/Si and GaP/Si [111] superlattices are presented, clearly showing 2D interface metallicity. Further, to investigate any possible superconductivity, the electron-phonon coupling constant, λ, is calculated within the crude rigid muffin-tin approximation (RMTA) (Ref. 17) and T_c is estimated using the McMillan formula.[18]

For all calculations, full structural optimization was performed, i.e., of the volume and internal coordinates, using the highly precise full-potential linearized augmented plane wave (FLAPW) (Refs. 19 and 20) method within the local-density approximation (LDA) to the exchange-correlation potential parametrized by Hedin and Lundqvist.[21] Now, ZnS and GaP crystallize in the zinc-blende structure with lattice constants 5.40 and 5.45 Å, respectively. We considered the

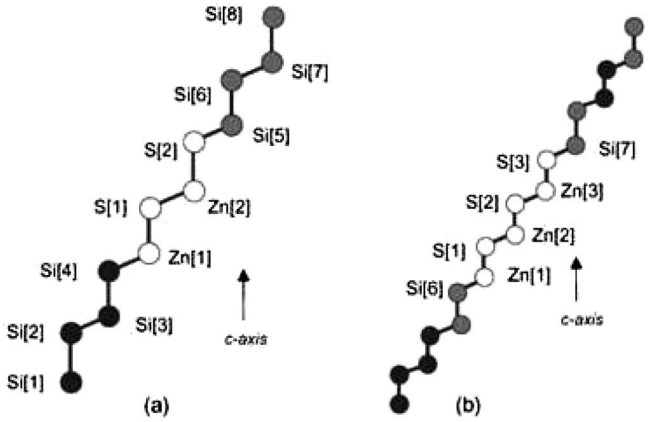

FIG. 1. Schematic drawing of ZnS/Si superlattice of (a) n=2 and (b) n=3 cases. GaP/Si superlattices have the same structure.

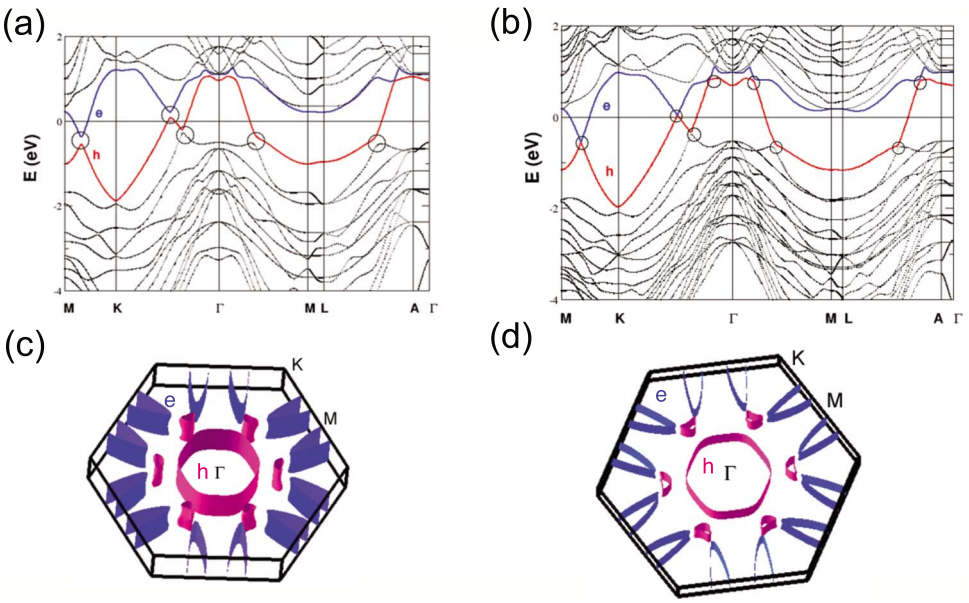

FIG. 2. (Color online) ZnS/Si superlattice. Band structure of (a) $n=2$ and (b) $n=3$ and corresponding Fermi-surface plots of (c) $n=2$ and (d) $n=3$, respectively. Label h (e) indicates hole (electron) band for each case. High symmetry points Γ, M, and K are shown in the Fermi-surface plots. Circled regions indicate where two interface bands anticross.

[111] growth direction of the superlattices A_n/Si_{4n} (A=GaP, ZnS) with $n=2,3$ layers. A schematic model for the ZnS/Si superlattices is sketched in Fig. 1. We used muffin-tin (MT) radii of 2.15 a.u. (for Zn and Ga) and 2.00 a.u. (for S, P, and Si), and spherical harmonics with $\ell \leq 8$ inside the MT spheres. The cutoff energy of the plane-wave basis was 12.96 Ry and that of the potential representation was 207.36 Ry. The improved tetrahedron method[22] was used for k point summations, with 119 points employed in the irreducible wedge of the Brillouin zone.

II. STRUCTURE AND LAYER-LAYER DISTANCES

The optimized lattice constants (a) and c/a ratios of the superlattices are shown in Table I. The numbers in parentheses are the relative changes (in percent) with respect to those of the bulk zinc-blende structures of ZnS and GaP. Here, the lattice constants are converted to those of the conventional zinc-blende structure for a better comparison. The c/a ratio without relaxation would be $\sqrt{6}\times n$ for n layers of ZnS or GaP, to which the c/a ratios of the relaxed structure are compared. In general, the changes in lattice constants and c/a ratios are small. This is not so for the interlayer distances. The comparison of layer-by-layer distances (in percent) before and after relaxation is summarized for ZnS/Si and GaP/Si in Tables II and III, respectively. Percentage changes of less than 4% are not listed except for the Ga[3]-P[3] layer in the $n=3$ GaP/Si superlattice. In the $n=2$ superlattices, both ZnS/Si and GaP/Si exhibit large changes in the layer-by-layer distance at the interfaces; the cation-Si distance increases while the anion-Si distance decreases. Moreover, the cation-anion distances in the ZnS or GaP region are considerably reduced. In the $n=3$ case, similar trends are observed in layer-by-layer distances but the

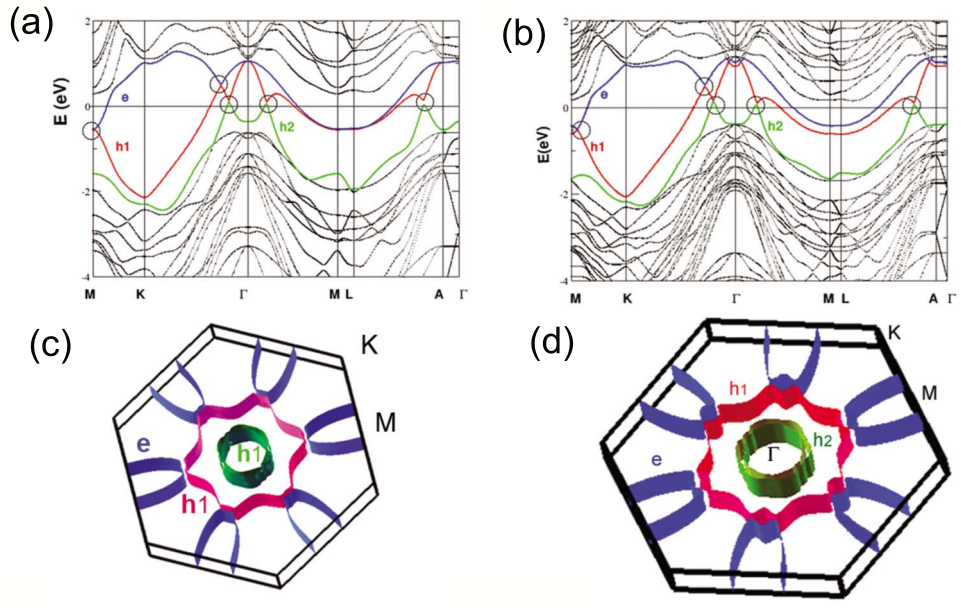

FIG. 3. (Color online) GaP/Si superlattices. Band structure of (a) $n=2$ and (b) $n=3$ and corresponding Fermi-surface plots of (c) $n=2$ and (d) $n=3$, respectively. Labels $h1$ and $h2$ (e) indicate hole (electron) band for each case. High symmetry points Γ, M, and K are shown in the Fermi-surface plots. Circled regions indicate where two interface bands anticross.

TABLE I. Optimized lattice constant (a) and c/a ratio for the superlattices. The lattice constants are converted to those of the zinc-blende structure. Numbers in parentheses are the relative changes (in %) of a and c/a with respect to those of zinc-blende structure without relaxation.

	$n=2$		$n=3$	
Superlattice	a (Å)	c/a	a (Å)	c/a
GaP/Si	5.41 (−0.7)	4.89 (−0.2)	5.40 (−0.9)	7.35 (0.0)
ZnS/Si	5.40 (0.0)	4.79 (−2.2)	5.40 (0.0)	7.30 (−0.7)

changes in the ZnS/Si superlattice are much larger than those in the GaP/Si.

III. TWO-DIMENSIONAL INTERFACE METALLICITY

Two dimensional interface metallicity is found in all superlattices. Plots of the band structures and Fermi surfaces are shown in Fig. 2 for ZnS/Si and in Fig. 3 for GaP/Si, with the electronlike and holelike bands indicated. The character of the electronlike band is mostly anion(sp)-Si(p) while that of the holelike band is cation(d)-Si(p). The dispersion of the bands looks quite similar at first glance but there are some noticeable differences: in the ZnS/Si case, both electronlike and holelike bands have dips along M-K which are not present in the GaP/Si case. The two anticrossings (circled) along K-Γ line fall above and below E_F in the ZnS/Si case while they are both above E_F in the GaP/Si case. This difference introduces six small hole pockets between Γ and K in the Fermi surface of the ZnS/Si superlattice, which are not present in the GaP/Si superlattices.

In the GaP/Si case there are two anticrossings (circled) very close to E_F that, along the Γ-M and L-A lines, are not present in the ZnS/Si case. This results in an additional holelike band (labeled as $h2$) both for the $n=2$ and $n=3$ cases. Another difference is that in the ZnS/Si case, the electronlike band does not cut the Γ-M line. In other words, it is above E_F along M-L, whereas in the GaP/Si case an electronlike band cuts Γ-M and is below E_F along M-L. This difference results in a different number of electronic sheets in the Fermi surface: the electron pockets consist of two sheets with six-fold symmetry in the ZnS/Si superlattice while in the GaP/Si superlattice they consist of a single sheet around M. In the band plots, band interactions are highlighted with circles at several points. An analysis on the symmetry of the wave functions as a function of k shows that all these are anticrossings. The splittings in the $n=3$ cases are smaller than those in the $n=2$ cases. Above all, the 2D character is clearly displayed in the shape of the Fermi surfaces and is additionally evidenced in the charge-density plots.

For states in the vicinity of E_F, within a slice of 0.075 eV, the charge densities are shown in Figs. 4 and 5 for the ZnS/Si and GaP/Si superlattices, respectively, for both the $n=2$ and

TABLE II. Percentage change in layer distances before and after relaxation for ZnS/Si superlattice. Changes of less than 4% are not listed here.

$n=2$		$n=3$	
Layer	Change (%)	Layer	Change (%)
Si[5]-S[2]	−26.97	Si[7]-S[3]	−28.75
Zn[2]-S[1]	−25.06	Zn[3]-S[2]	−17.15
Zn[1]-Si[4]	10.28	Zn[2]-S[1]	−14.26
		Zn[1]-Si[6]	20.41

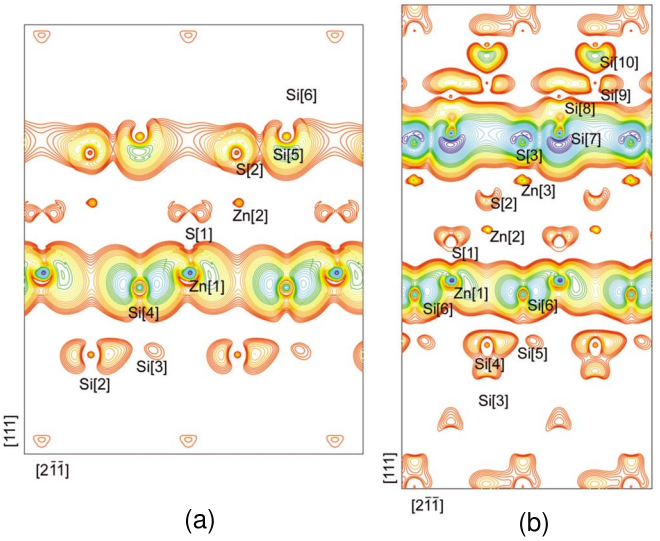

FIG. 4. (Color online) Charge-density contour plots of (a) $n=2$ and (b) $n=3$ ZnS/Si superlattices around E_F within an energy slice of 0.075 eV. The starting density is 5.0×10^{-4} e/bohr^3 and subsequent lines increase by a factor of 1.15.

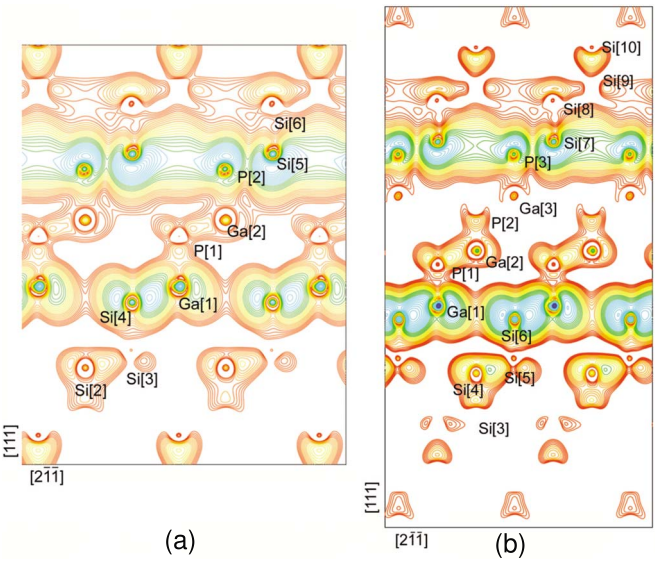

FIG. 5. (Color online) Charge-density contour plots of (a) $n=2$ and (b) $n=3$ GaP/Si superlattices around E_F within an energy slice of 0.075 eV. The starting density is 1.0×10^{-3} e/bohr^3 and subsequent lines increase by a factor of 1.15.

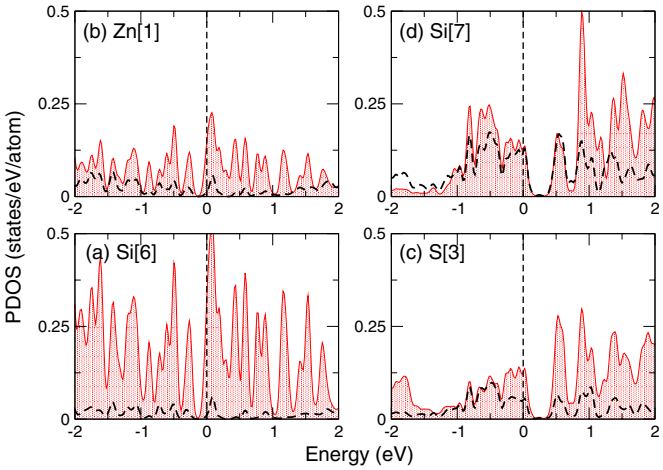

FIG. 6. (Color online) pDOS around the Fermi energy for the $n=3$ ZnS/Si superlattice for the interface atoms (Si[6], Zn[1], S[3], and Si[7]). (a) Si[6], (b) Zn[1], (c) S[3], and (d) Si[7]. The s orbitals are shown in black dashed lines; the p orbitals by a (red) solid line and shaded. The Fermi energy is indicated by the vertical dotted line.

$n=3$ cases. The highest concentration of charge is at the interfaces, with the charge in GaP/Si being more spread out in the c direction from the interfaces than in ZnS/Si. However, the charge-density plots in both cases exhibit qualitatively similar trends, i.e., the interfaces can be thought as a metallic slab sandwiched by dielectric layers (the ZnS or GaP regions). The interface metallicity is also well demonstrated in the partial density of states (pDOS) plots in Figs. 6 and 7, where the pDOS of the interface atoms is plotted near the Fermi energy. The p-type interfaces have more localized features than the n-type interfaces, as seen in the pDOS plots and the charge-density plots. The character of the interface states is mostly p states hybridized with s states.

For a quantitative analysis of the interface charge, relative changes (in percent) of the MT charge with respect to their

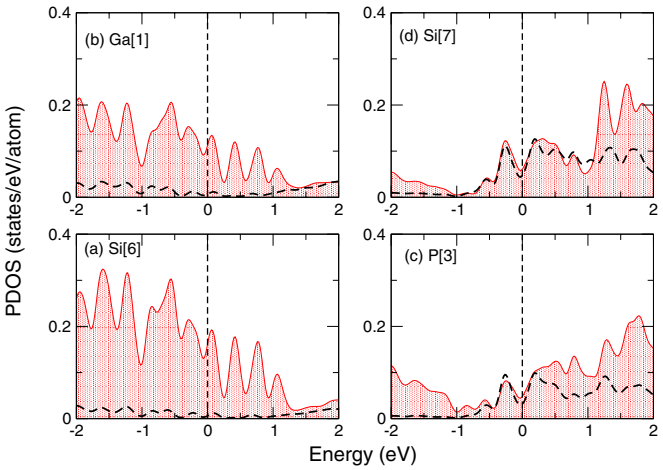

FIG. 7. (Color online) pDOS around the Fermi energy for the $n=3$ GaP/Si superlattice for the interface atoms (Si[6], Ga[1], P[3], and Si[7]). (a) Si[6], (b) Ga[1], (c) P[3], and (d) Si[7]. The s orbitals are shown in black dashed lines; the p orbitals by a (red) solid line and shaded. The Fermi energy is indicated by the vertical dotted line.

TABLE III. Percentage change in layer distances before and after relaxation for GaP/Si superlattice. Changes of less than 4% are not listed here.

$n=2$		$n=3$	
Layer	Change (%)	Layer	Change (%)
Si[5]-P[2]	−26.89	Si[7]-P[3]	−5.85
Ga[2]-P[1]	−24.98	Ga[3]-P[3]	2.02
Ga[1]-Si[4]	10.40	P[2]-Ga[3]	4.91
		Ga[1]-Si[6]	5.36

bulk counterparts are listed in Tables IV and V for the ZnS/Si and the GaP/Si superlattices, respectively. The interface Si atoms lose charge while the interface Zn/Ga and S/P gain charge. The changes in the ZnS/Si superlattices are generally larger than in the GaP/Si superlattices. If one assumes the two-electron-per-bond counting rule, the Si-Zn (Si-Ga) bond lacks 2/4 (1/4) electron per bond while the Si-S (Si-P) bond has an excess of 2/4 (1/4) electron. This simple counting rule explains the p-type character of the Si-Zn (Si-Ga) interfaces and the n-type character of the Si-S (Si-P) interfaces. The larger charge imbalance in the ZnS/Si superlattice compared to GaP/Si, due to the larger polarity mismatch with Si atoms, yields larger changes in MT charge as well as stronger confinement of the conducting electrons at the interfaces.

IV. SUPERCONDUCTIVITY

To explore superconductivity, first the McMillan-Hopfield[18,23] electron-phonon coupling constant, λ_{ep}, is calculated within the crude RMTA.[17] The average phonon frequency is estimated by $\langle\omega^2\rangle^{1/2}=0.69\langle\Theta_D\rangle$, where Θ_D is the weighted average of Θ_D for Si and ZnS (GaP). The experimental Debye temperatures taken for the calculations are 625,[24] 440,[25] and 445 K (Ref. 26) for Si, ZnS, and GaP, respectively. The average $\langle\Theta_D\rangle$, the estimated λ_{ep}, and the Coulomb pseudopotential, $\mu^\star$, are given in Table VI, with $\mu^\star$ evaluated using the simple formula by Bennemann and Garland.[27] Then T_c is estimated using the McMillan formula.[18] The electron-phonon coupling is seen to be strongest at the interfaces; however, as can be easily verified, the resulting T_c's are less than 10^{-5} K. Therefore, in ZnS/Si and GaP/Si superlattices, superconductivity within the electron-phonon mediation scheme is unlikely.

TABLE IV. Relative change (in %) of the orbital-resolved MT charge of the interface atoms in ZnS/Si superlattices with respect to bulk Si and ZnS.

$n=2$	s	p	d	$n=3$	s	p	d
Si[4]	7.83	−9.51		Si[6]	8.18	−11.81	
Zn[1]	28.51	16.93	−0.66	Zn[1]	26.25	11.76	−0.63
S[2]	4.33	−2.93		S[3]	4.46	−2.88	
Si[5]	11.62	−17.38		Si[7]	11.95	−17.68	

TABLE V. Relative change (in %) of the orbital-resolved MT charge of the interface atoms in GaP/Si superlattices with respect to bulk Si and GaP.

$n=2$	s	p	d	$n=3$	s	p	d
Si[4]	4.55	−2.13		Si[6]	4.75	−2.82	
Ga[1]	7.56	8.38	−0.18	Ga[1]	7.34	7.93	−0.18
P[2]	2.04	−3.51		P[3]	2.14	−3.46	
Si[5]	3.27	−11.28		Si[7]	3.39	−11.02	

TABLE VI. Average Debye temperature ($\langle\Theta_D\rangle$), calculated electron-phonon coupling constant (λ), and Coulomb pseudopotential ($\mu^\star$) for ZnS/Si and GaP/Si superlattices.

	ZnS/Si		GaP/Si	
	$n=2$	$n=3$	$n=2$	$n=3$
$\langle\Theta_D\rangle$	588	588	589	589
λ	0.075	0.098	0.043	0.042
$\mu^\star$	0.04	0.028	0.029	0.023

V. DISCUSSION

In summary, we presented a study of the heterobonded semiconductor superlattices, ZnS/Si and GaP/Si. All superlattices clearly exhibit 2D metallicity at the interfaces, as shown by the band structures, Fermi surfaces, charge-density plots, and pDOS. What is remarkable is that there is interface metallicity while their bulk counterparts (Si, GaP, and ZnS) are all insulating, with band gaps of 1.17, 2.32, and 3.91 eV, respectively. Note that the CuCl/Si and $LaAlO_3/SrTiO_3$ superlattices also exhibit metallicity at the interfaces,[3,4,16] whereas the bulk materials are insulators. What is common in all these superlattices is that the polarity mismatch results in interface 2D metallicity. The possibility of phonon-mediated superconductivity of the ZnS/Si and GaP/Si superlattices was investigated using the crude RMTA method. The largest electron-phonon coupling in all these superlattices is at the interfaces. However, whereas the CuCl/Si superlattices were found to be possible superconductors within the BCS electron-phonon-mediated scheme (with T_c between 0.3 and 4 K), the RMTA calculation suggests no superconductivity in the ZnS/Si and GaP/Si cases. Nevertheless, with the exciton mechanism in mind, an intriguing and potentially important 2D metallicity is found at the interfaces of these valence mismatched semiconductors. Moreover, the interface metallic regions separated by semiconducting bulk regions can be viewed as a dielectric-metal-dielectric sandwich structure—the geometry proposed by Ginzburg[13] for exciton-mediated superconductivity.

ACKNOWLEDGMENTS

This work was supported by the U.S. Department of Energy (Grant No. DE-FG02-88ER 45372/A021 and a supercomputing time grant at NERSC). S.H.R. thanks Michael Weinert for helpful assistance.

*Department of Physics, University of Wisconsin-Milwaukee, WI, 53211.
†Department Fysica, Universiteit Antwerpen, B-2020 Antwerpen, Belgium.

[1] W. A. Harrison, E. A. Kraut, J. R. Waldrop, and R. W. Grant, Phys. Rev. B **18**, 4402 (1978).
[2] A. Ohtomo, D. A. Muller, J. L. Grazul, and H. Y. Hwang, Nature (London) **419**, 378 (2002).
[3] A. Ohtomo and H. Y. Hwang, Nature (London) **427**, 423 (2004).
[4] M. S. Park, S. H. Rhim, and A. J. Freeman, Phys. Rev. B **74**, 205416 (2006).
[5] N. Reyren *et al.*, Science **317**, 1196 (2007).
[6] B. Mattes and C. Foiles, Physica B & C **135B**, 139 (1985).
[7] C. W. Chu, A. P. Rusakov, S. Huang, S. Early, T. H. Geballe, and C. Y. Huang, Phys. Rev. B **18**, 2116 (1978).
[8] N. B. Brandt, S. V. Kuvshinnikov, A. P. Rusakov, and V. M. Semenov, JETP Lett. **27**, 33 (1978).
[9] A. A. Abrikosov, JETP Lett. **27**, 219 (1978).
[10] W. Little, Phys. Rev. **134**, A1416 (1964).
[11] V. L. Ginzburg, Sov. Phys. JETP **20**, 1549 (1965).
[12] B. L. Mattes, Physica C **162-164**, 554 (1989).
[13] V. Ginzburg, Contemp. Phys. **9**, 355 (1968).
[14] D. Allender, J. Bray, and J. Bardeen, Phys. Rev. B **7**, 1020 (1973).
[15] J. Yu and A. J. Freeman, Army Research Conference, New Jersey, 15 December 1986 (unpublished).
[16] S. H. Rhim, R. Saniz, J. Yu, L.-H. Ye, and A. J. Freeman, Phys. Rev. B **76**, 184505 (2007).
[17] G. D. Gaspari and B. L. Gyorffy, Phys. Rev. Lett. **28**, 801 (1972).
[18] W. L. McMillan, Phys. Rev. **167**, 331 (1968).
[19] E. Wimmer, H. Krakauer, M. Weinert, and A. J. Freeman, Phys. Rev. B **24**, 864 (1981).
[20] H. J. F. Jansen and A. J. Freeman, Phys. Rev. B **30**, 561 (1984).
[21] L. Hedin and B. I. Lundqvist, J. Phys. C **4**, 2064 (1971).
[22] P. E. Blöchl, O. Jepsen, and O. K. Andersen, Phys. Rev. B **49**, 16223 (1994).
[23] J. J. Hopfield, Phys. Rev. **186**, 443 (1969).
[24] N. W. Ashcroft and N. D. Mermin, *Solid State Physics* (Holt, Rinehart and Winston, New York, 1976).
[25] *Numerical data and functional relationships in Science and Technology*, Landolt-Börnstein, New Series, Group III, edited by O. Madelung, Vol. 22 (Springer, Berlin, 1989).
[26] http://www.ioffe.ru/SVA/NSM/
[27] K. Bennemann and J. Garland, in *Superconductivity in d- and f-band Metals*, AIP Conf. Proc. No. 3, edited by D. H. Douglas (AIP, New York, 1972), p. 103.